

Supplementary Information

Multifunctional additive enables all-polymer solar cells with improved efficiency, photostability and mechanical durability

Jiali Song,^a Linglong Ye,^{*a} Chunhui Liu,^a Yunhao Cai,^a Chen Zhang,^a GuiChu Yue,^a Yun Li,^a Min Hun Jee,^b Yong Zhao,^a Donghui Wei,^c Han Young Woo,^b Yanming Sun^{*a}

^aSchool of Chemistry, Beihang University, Beijing 100191, P. R. China, E-mail: sunym@buaa.edu.cn.

^bDepartment of Chemistry, College of Science, KU-KIST Graduate School of Converging Science and Technology, Korea University, Seoul 136-713, Republic of Korea.

^cCollege of Chemistry and Molecular Engineering, Zhengzhou University, Zhengzhou 450001, P. R. China.

Materials and Reagents

PM6 ($M_n = 35.1$ kDa, $M_w = 51.1$ kDa, PDI = 1.46)¹ was purchased from Solarmer Materials Inc. (Beijing, China). PY-C11 ($M_n = 9.3$ kDa, $M_w = 18.6$ kDa, PDI = 2.00), PY-DT ($M_n = 10.2$ kDa, $M_w = 23.6$ kDa, PDI = 2.31) and PYF-T-*o* ($M_n = 10.5$ kDa, $M_w = 17.7$ kDa, PDI = 1.68) were synthesized by our group according to the reported works.²⁻⁴ Chloroform (CF) was purchased from Sigma Aldrich. 2-Methoxynaphthalene (2-MN) was purchased from Aladdin.

Synthesis of DTC solid additives

Octane-1,12-diyl bis(thiophene-3-carboxylate) (DTC-C8)

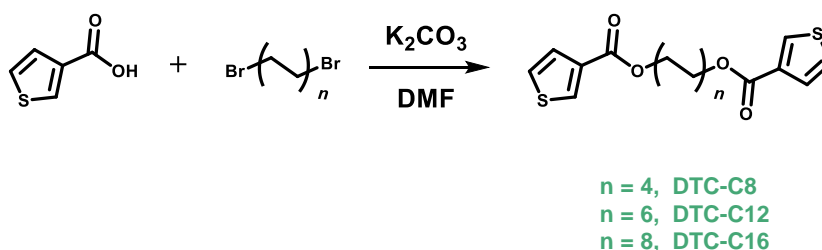
A single-neck round flask was charged with thiophene-3-carboxylic acid (1.00 g, 7.80 mmol), 1,12-dibromododecane (1.06 g, 3.90 mmol, 0.5 eq) and K_2CO_3 (1.29 g, 9.36 mmol, 1.2eq) in 10 mL DMF. After stirring for 6 hours at 50 °C, the reaction mixture was poured into water and extracted with dichloromethane (DCM). The organic layer was dried over Na_2SO_4 , filtered and concentrated. The residue was purified with silica gel chromatography (eluent: petroleum ether/DCM, *v/v*, 2:1) to provide pure product as white solid (1.36 g, 95%). ¹H NMR (400 MHz, $CDCl_3$) δ 8.14-8.04 (m, 2H), 7.57-7.47 (m, 2H), 7.30 (dd, $J = 5.1, 3.1$ Hz, 2H), 4.27 (t, $J = 6.7$ Hz, 4H), 1.74 (p, $J = 6.8$ Hz, 4H), 1.50-1.29 (m, 8H). MALDI-TOF MS: Calcd. for $C_{18}H_{22}O_4S_2Na$ [$M + Na$]⁺, Exact Mass: 389.085; Found: 388.969.

Dodecane-1,12-diyl bis(thiophene-3-carboxylate) (DTC-C12)

Synthesis of DTC-C12 was carried out in a similar manner to that of DTC-C8. ¹H NMR (400 MHz, $CDCl_3$) δ 8.10 (dd, $J = 3.1, 1.2$ Hz, 2H), 7.52 (dd, $J = 5.0, 1.2$ Hz, 2H), 7.30 (dd, $J = 5.0, 3.1$ Hz, 2H), 4.26 (t, $J = 6.7$ Hz, 4H), 1.73 (p, $J = 6.9$ Hz, 4H), 1.46-1.23 (m, 16H). MALDI-TOF MS: Calcd. for $C_{22}H_{30}O_4S_2Na$ [$M + Na$]⁺, Exact Mass: 445.147; Found: 445.040.

Cetane-1,12-diyl bis(thiophene-3-carboxylate) (DTC-C16)

Synthesis of DTC-C16 was carried out in a similar manner to that of DTC-C8. ¹H NMR (400 MHz, $CDCl_3$) δ 8.08 (d, $J = 3.1$ Hz, 2H), 7.51 (d, $J = 5.0$ Hz, 2H), 7.29 (t, $J = 4.1$ Hz, 2H), 4.25 (t, $J = 6.7$ Hz, 4H), 1.72 (p, $J = 7.0$ Hz, 4H), 1.47-1.01 (m, 24H). MALDI-TOF MS: Calcd. for $C_{26}H_{38}O_4S_2Na$ [$M + Na$]⁺, Exact Mass: 501.210; Found: 501.117.



Scheme S1. Synthetic routes of DTC-C8, DTC-C12 and DTC-C16.

Device fabrication

All-polymer solar cells (all-PSCs) were fabricated with a device structure of ITO/PEDOT:PSS/PM6:polymer acceptors/PNDIT-F3N/Ag. The ITO-coated substrates were sequentially cleaned by detergent deionized water, acetone, and isopropyl alcohol for 20 min in ultrasonic cleaning machine. The cleaned ITO-coated substrates were dried in an oven at 100 °C overnight. Before used, the ITO-coated substrates were pretreated by a plasma cleaner for 2 min under a vacuum condition of 10 Pa. A 40 nm thick of PEDOT:PSS layer was firstly spin cast on top of the ITO substrates at a rate of 4000 rpm for 30 s and followed by thermal annealing at 150 °C for 10 min under ambient conditions. The active layer solution was prepared by dissolved PM6 and polymer acceptors with a weight ratio of 1:1 and a total concentration of 12 mg/mL in CF solvent. 2-MN (150% to the total mass of PM6:polymer acceptors) was used as volatile solid additive. The optimal content of DTC non-volatile solid additive is 3% of the total mass of PM6:polymer acceptors. The CF solutions were stirred at normal temperature (25 °C) for 4 hours before used. The active layers were generated by spin-coating the CF solution on the top of PEDOT:PSS layer for 30 s at a rate of 2500 rpm with an optimal thickness of 110 nm under nitrogen atmosphere. Then, the active layers were all thermally annealed at 80 °C for 8 min. Subsequently, a PNDIT-F3N layer with a concentration of 1.2 mg/mL in mixed solvent (methanol:acetic acid is 200:1 by volume) was spin-coated onto the active layer at a rate of 4200 rpm for 30 s. Finally, 120 nm Ag electrode were deposited under a vacuum condition of 2×10^{-4} Pa. The active area of devices is 5.12 mm². The devices were tested through a mask with an area of 3.15 mm².

Device characterizations

Device performance was measured by using a 510 Air Mass 1.5 Global (AM1.5G) solar simulator (SS-F5-3A, Enlitech) with an irradiation intensity of 100 mW cm^{-2} , determined by using a calibrated silicon solar cell (SRC2020, Enlitech). J - V characteristics were measured by using a Keithley 2400 Source Measure Unit. EQE spectra were performed by using a QE-R3011 Solar Cell EQE measurement system (Enlitech). The UV-vis absorption spectra were measured by using Shimadzu (model UV-3700) UV-vis spectrophotometer. The hole-only devices with a structure of ITO/PEDOT:PSS/active layer/ MoO_3 /Ag, and electron-only devices with a structure of ITO/ ZnO /active layer /PNDIT-F3N/Ag were fabricated and tested under dark condition. The mobilities were determined by fitting corresponding J - V characteristics by using the equation of $J = (9/8)\epsilon_r\epsilon_0\mu(V^2/L^3)$, where J is the current density, ϵ_r is the dielectric permittivity of the transport medium, ϵ_0 is the vacuum permittivity of free space, L is the thickness of the active layer, and μ is the mobility. $V = V_{\text{app}} - V_{\text{bi}}$, where V_{app} is the applied voltage, V_{bi} is the offset voltage (V_{bi} is 0 V here). Atomic force microscope (AFM) was performed on a Dimension Icon AFM (Bruker) using tapping mode. GIWAXS measurements were carried out at the PLS-II 9A U-SAXS beamline of the Pohang Accelerator Laboratory in Korea. Contact angle (CA) measurements were performed by JC200D3M and the surface tension (γ) values of the neat films were determined by Wu's model through the contact angles of based on water and glycerol drop. Differential scanning calorimetry (DSC) measurements were carried by Mettler DSC3, the samples were all treated at a heating and cooling rate of $15 \text{ }^\circ\text{C min}^{-1}$ under nitrogen atmosphere. The Flory-Huggins interaction parameter (χ) values were determined by the melting point depression data of the DSC curves through the equation of $1/T_m - 1/T_m^0 = -Rv_2/\Delta H_{f1}[\ln\Phi_2/m_2 + (1/m_2 - 1/m_1) \times (1 - \Phi_2) + \chi(1 - \Phi_2)^2]$,⁵ where T_m and T_m^0 are the melting points of the blends and the neat higher crystalline material, R is ideal gas constant. The subscript 1 and 2 represent PY-C11 and PM6, respectively. v is the molar volume of the repeating units. Φ is the volume fraction and m is the degree of polymerization of each polymer component.

Device photostability characterizations

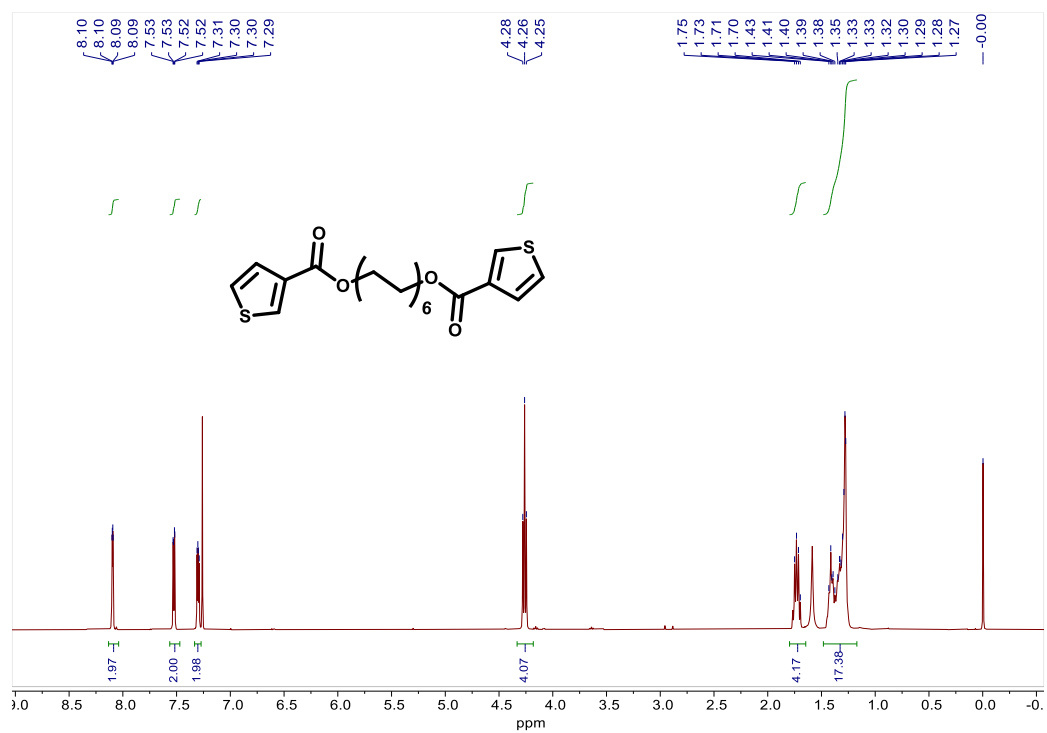
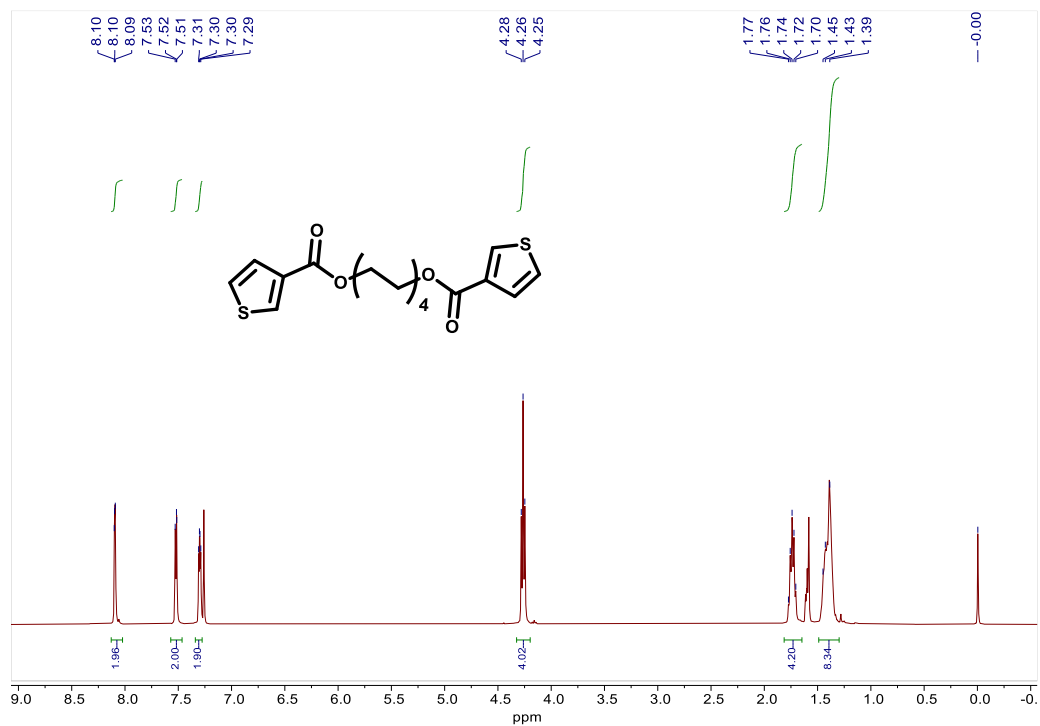
The photostability data were collected from five independent devices by using Maximum Power Point (MPP) tracking mode (YH-VMPP-IV-16). The devices were prepared in the same batch and encapsulated under the same conditions. Then, the photostability of these encapsulated devices were

measured under continuous LED light source (380-810 nm, one solar intensity) at the same time in ambient air conditions (the average humidity was 40%, the average tested temperature was 45 °C). The device encapsulation process is shown as follow: Firstly, a layer of UV-curable adhesive was evenly smeared on the electrode surface of device in the N₂ atmosphere. Then, a piece of coverslip was put on the top of adhesive. Finally, the device was illuminated under UV light source (365 nm) for 5 minutes. The aging measurements such as aging UV-vis absorption and GIWAXS of the blends, aging V_{oc} versus P_{light} curves of the devices are shown as follow: all the samples were measured before and after LED light illumination (one-sun intensity) for 192 h under ambient air conditions (the average humidity was 55%, the average tested temperature was 48 °C), which are nearly the same to the test conditions of photostability measurement.

Working mechanism analysis

The DFT calculations were performed using the Gaussian 09 program. The geometry optimizations were carried out by using the B3LYP functional and 6-31+G(d, p) basis set. FT-IR spectra were measured by Thermo Scientific Nicolet iS5.

Figures and Tables



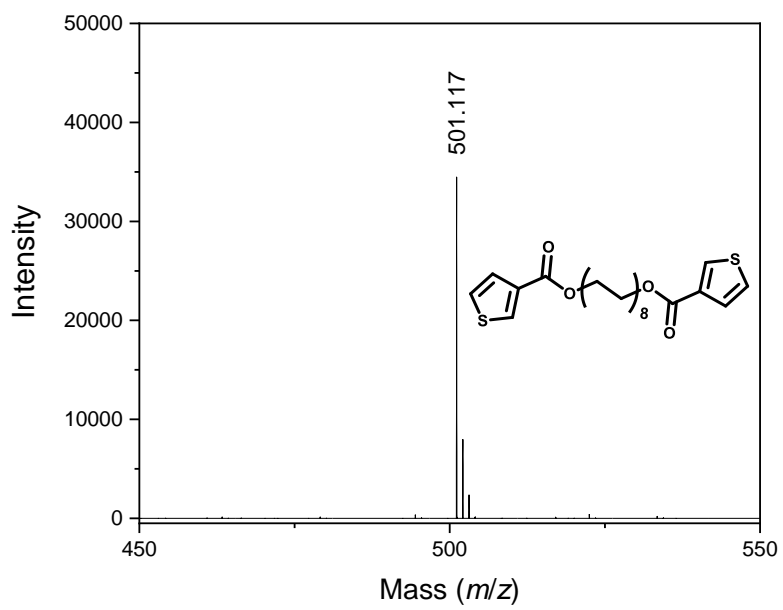
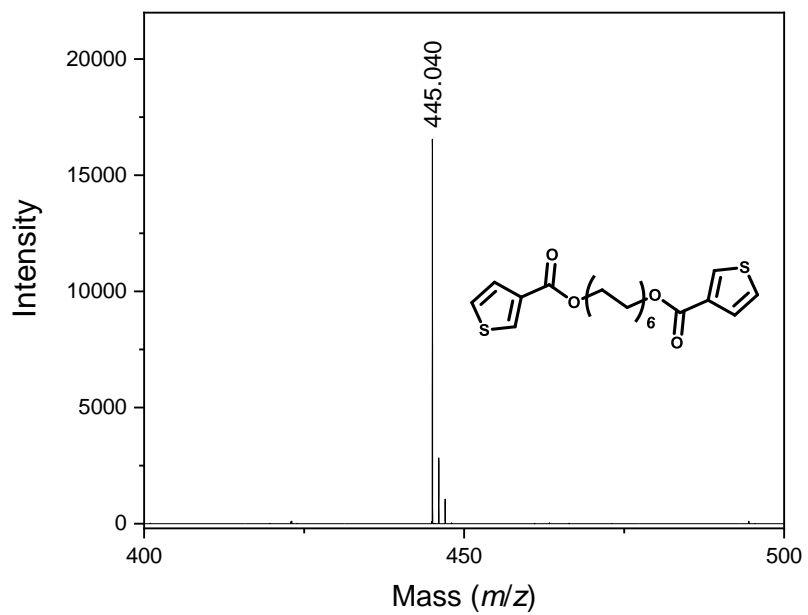


Fig. S2 MALDI-TOF spectra of DTC-C8, DTC-C12 and DTC-C16.

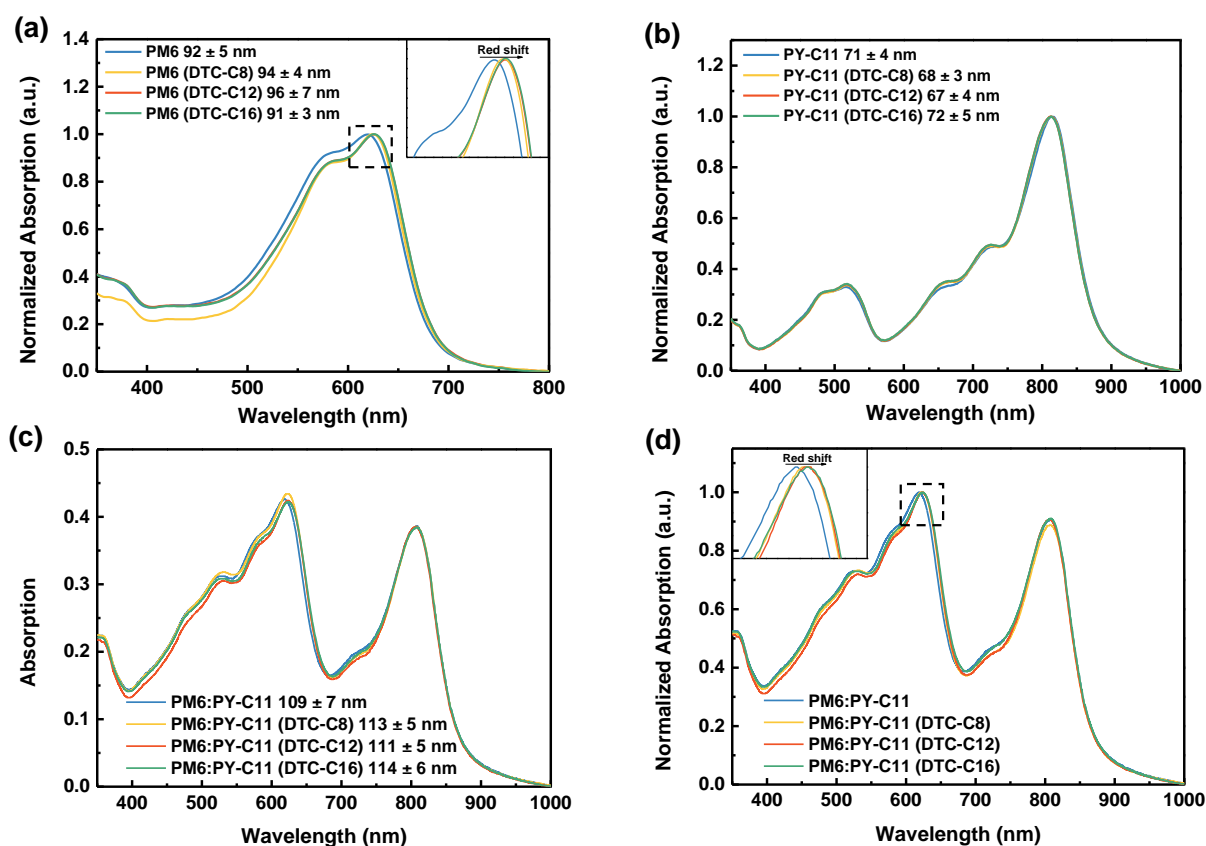


Fig. S3 (a, b) Normalized UV-vis absorption of PM6 and PY-C11 neat films processed with and without DTC additives and the corresponding film thickness. (c, d) Non-normalized and normalized UV-vis absorption of PM6:PY-C11 blend films processed with and without DTC additives and the corresponding film thickness.

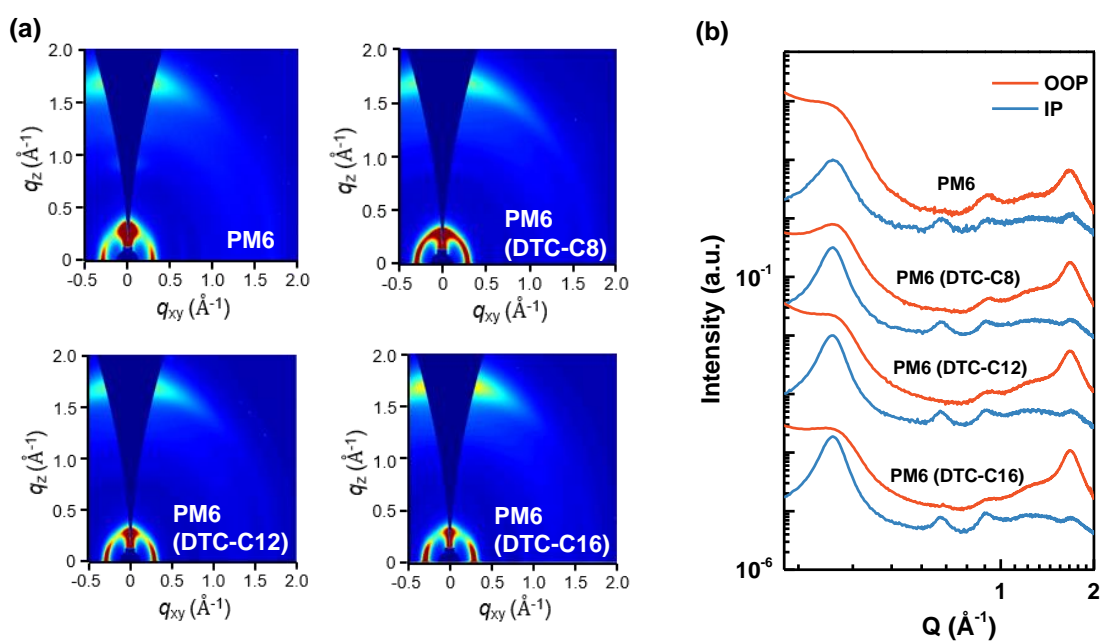


Fig. S4 (a) 2D GIWAXS diffraction patterns and (b) corresponding line-cut profiles of PM6 neat films processed without or with DTC additives with different alkyl chain length.

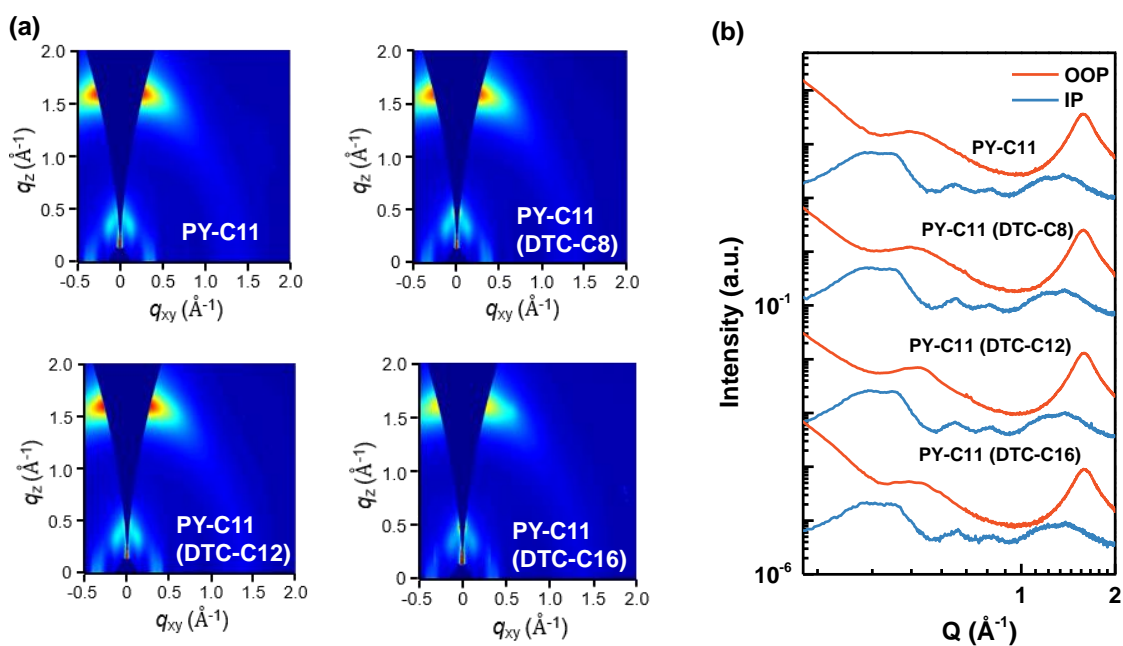


Fig. S5 (a) 2D GIWAXS diffraction patterns and (b) corresponding line-cut profiles of PY-C11 neat films processed without or with DTC additives with different alkyl chain length.

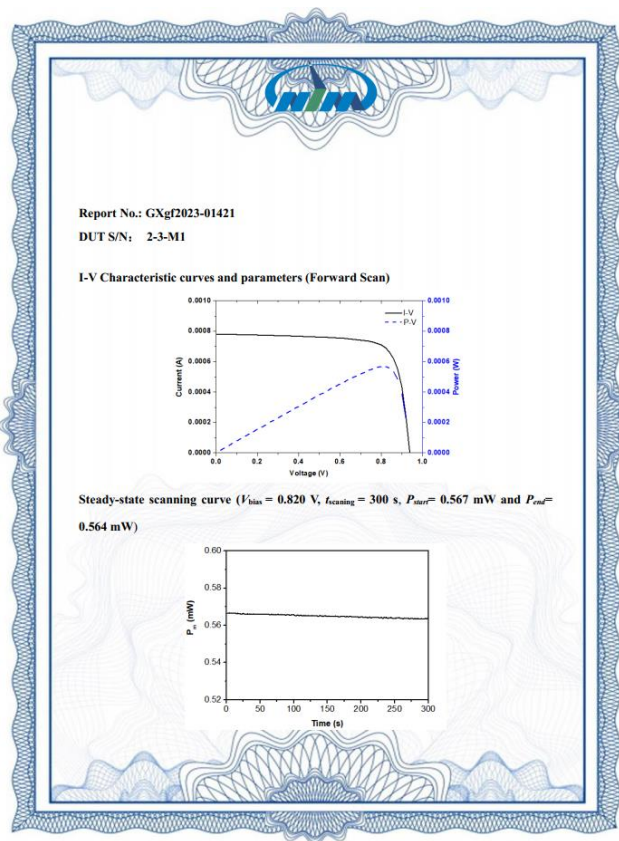
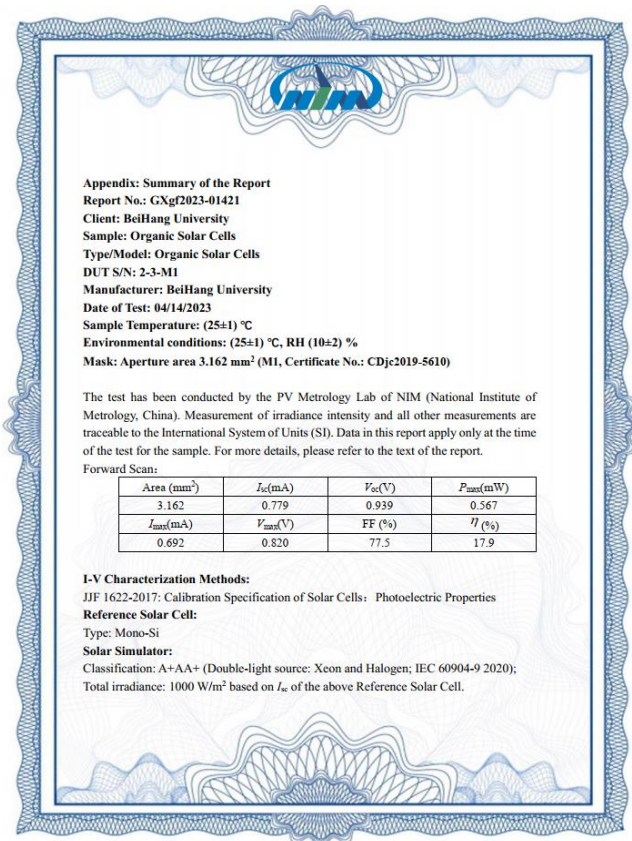


Fig. S6 The certification report for the DTC-C12-processed PM6:PY-C11 device from National Institute of Metrology (NIM), China.

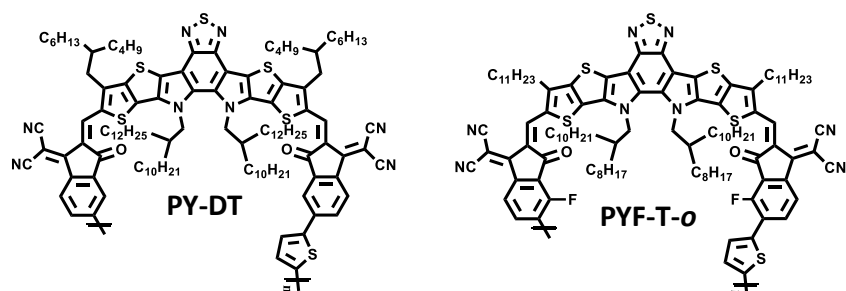


Fig. S7 Chemical structures of PY-DT and PYF-T-o.

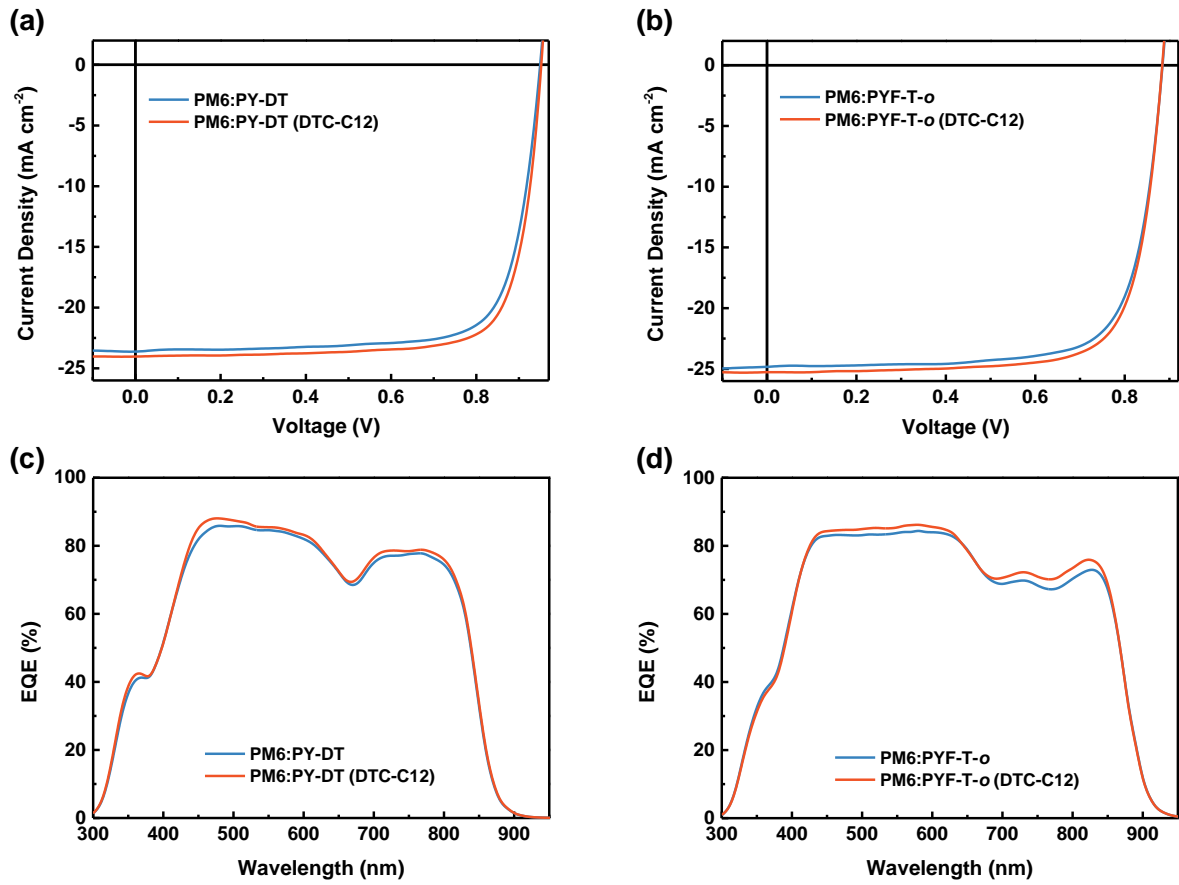


Fig. S8 (a-b) $J-V$ characteristics and (c-d) the corresponding EQE spectra of the PM6:PY-DT and PM6:PYF-T-o devices processed without and with DTC-C12.

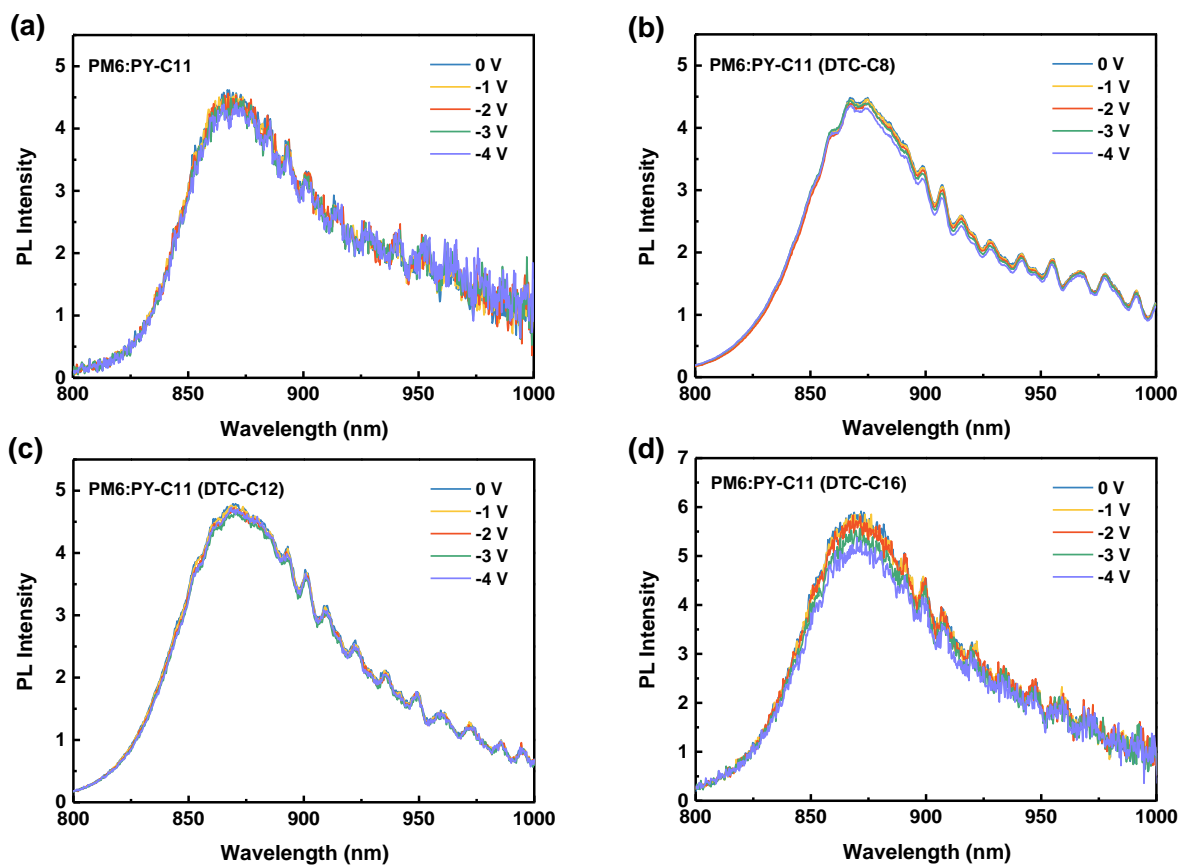


Fig. S9 Bias-dependent PL of the PM6:PY-C11 blend films processed with and without DTC additives.

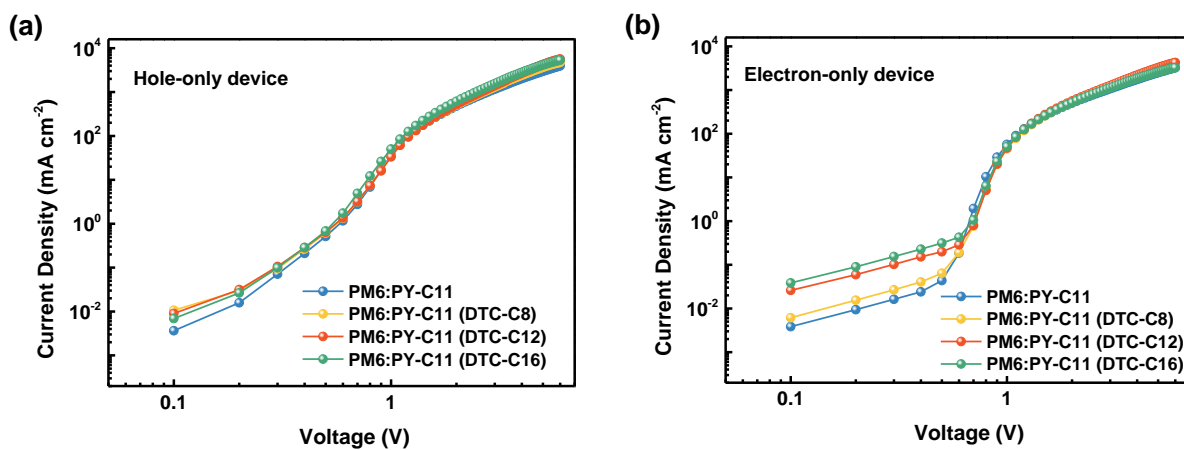


Fig. S10 SCLC curves of (a) hole-only devices and (b) electron-only devices processed without DTC additives and with DTC-C8, DTC-C12 and DTC-C16.

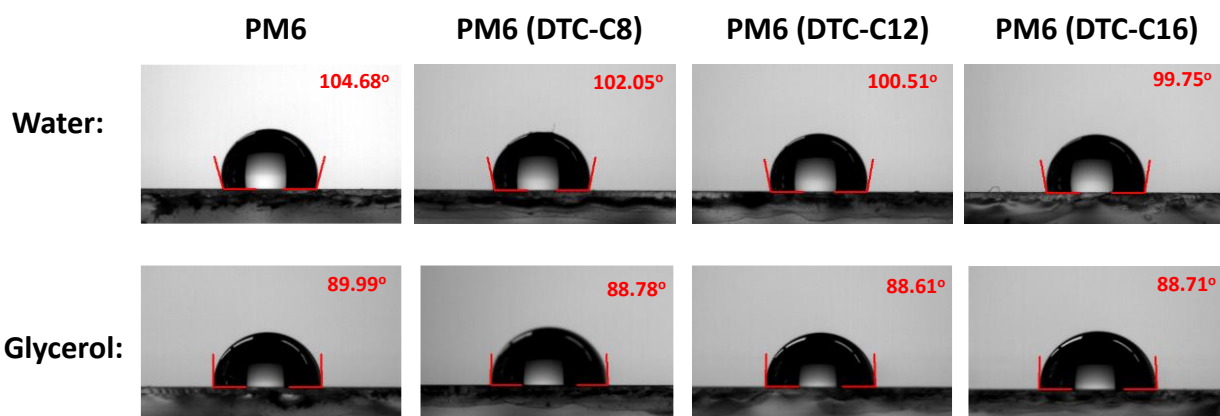


Fig. S11 Contact angles of PM6, PM6 (DTC-C8), PM6 (DTC-C12) and PM6 (DTC-C16) neat films based on water and glycerol drops.

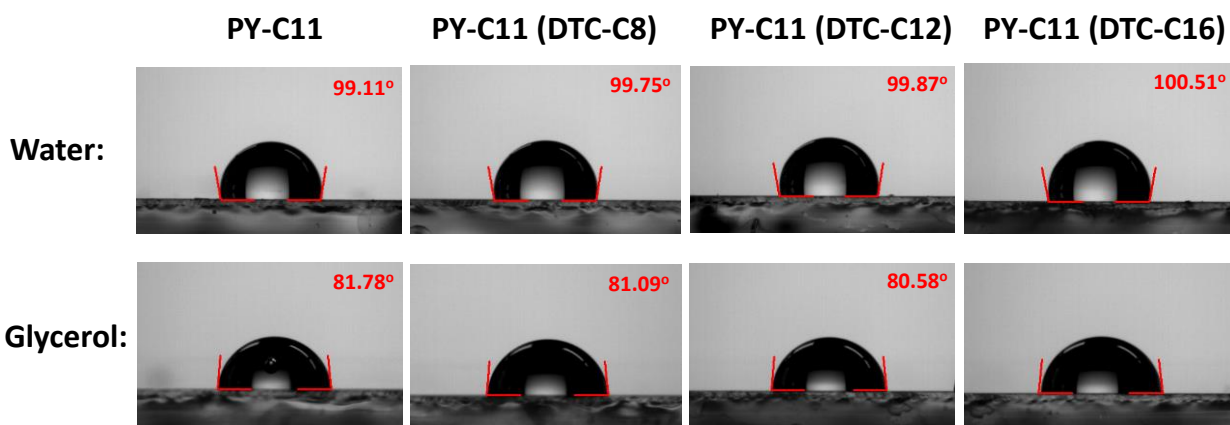


Fig. S12 Contact angles of PY-C11, PY-C11 (DTC-C8), PY-C11 (DTC-C12) and PY-C11 (DTC-C16) neat films based on water and glycerol drop.

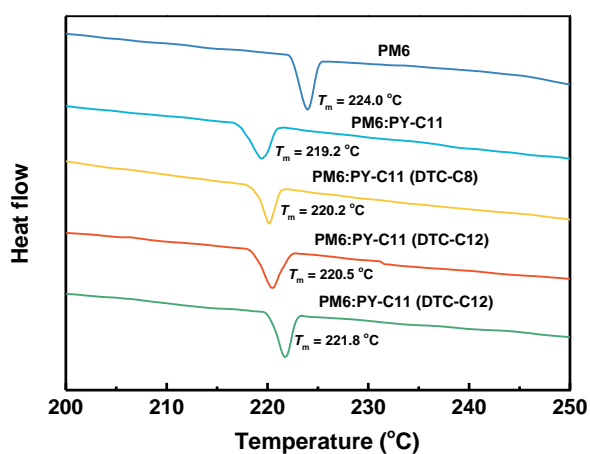


Fig. S13 DSC curves of PM6 and PM6:PY-C11 blends with and without DTC additives.

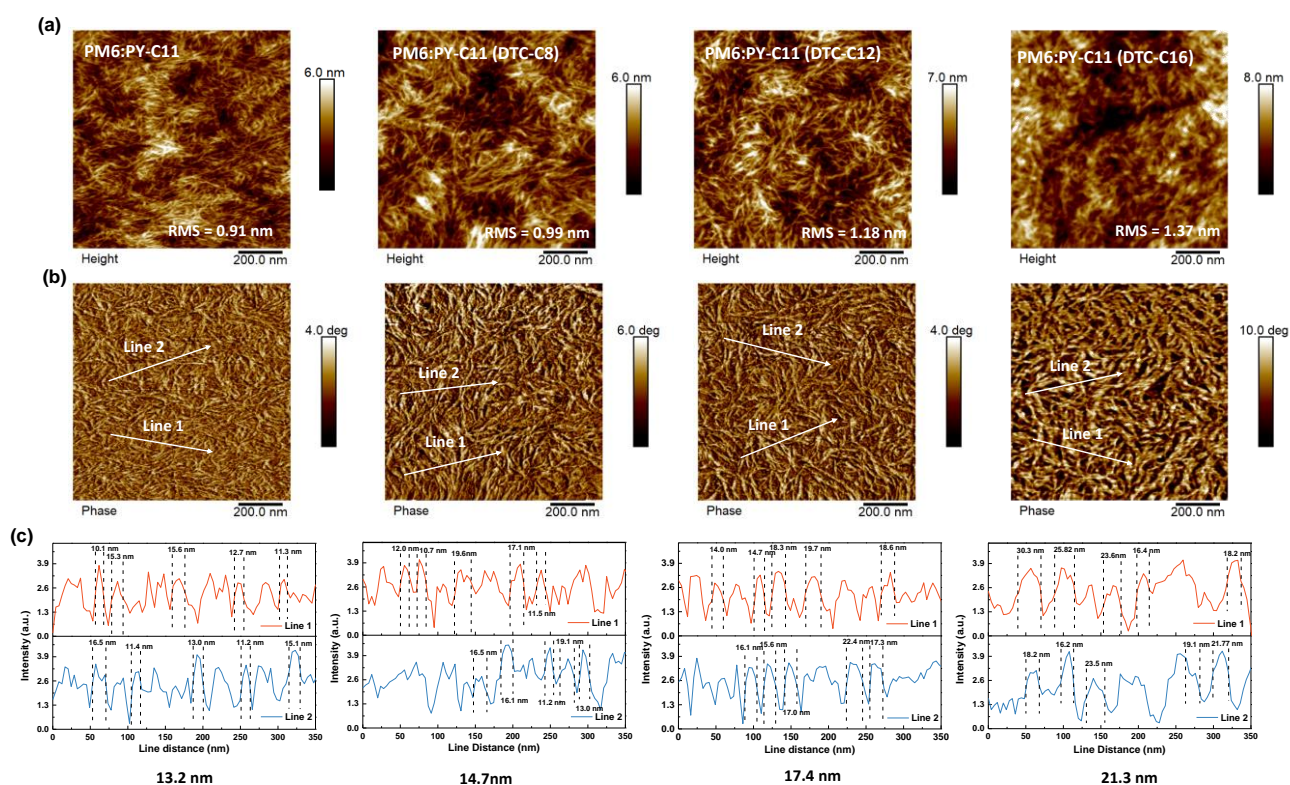


Fig. S14 AFM (a) height and (b) phase images of PM6:PY-C11 blend films processed without DTC additives and with DTC-C8, DTC-C12 and DTC-C16. (c) The line profiles to obtain the FWHM of cross-sections through AFM signals of blend films processed without DTC additives and with DTC-C8, DTC-C12 and DTC-C16.

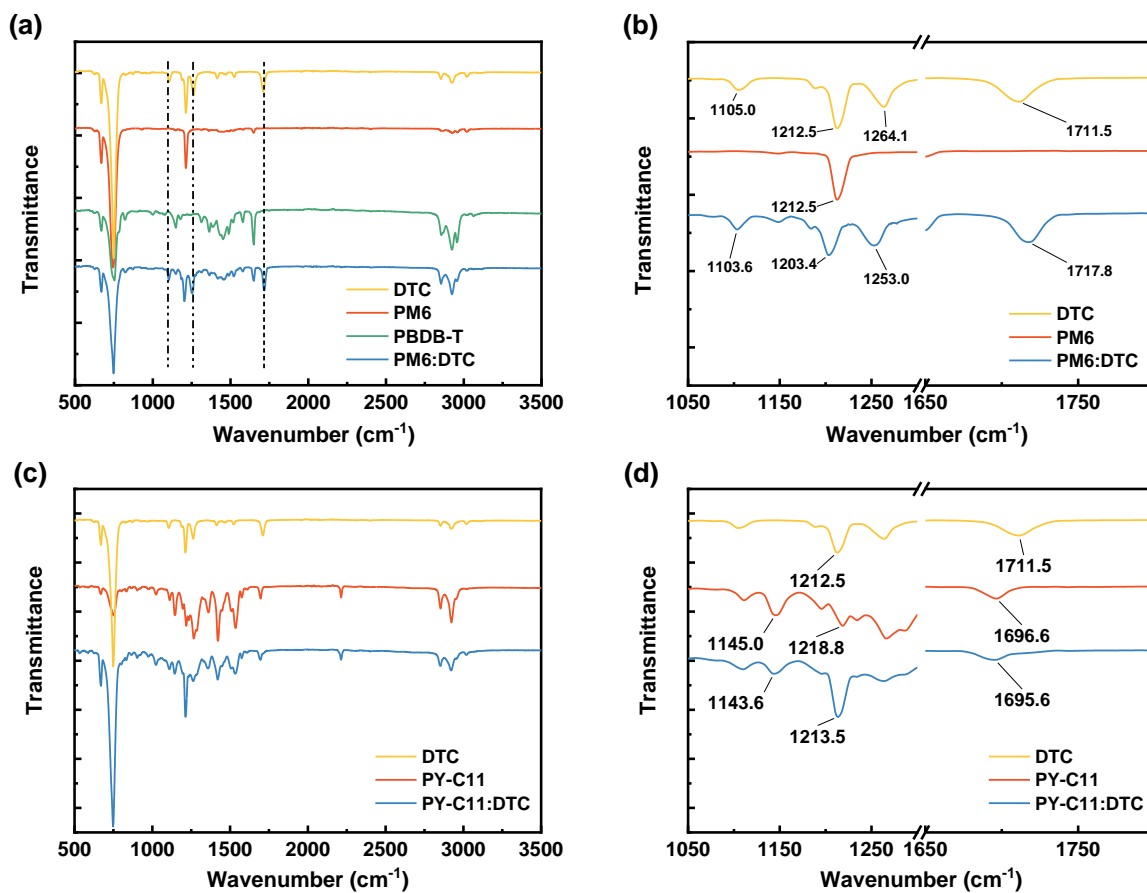


Fig. S15 FT-IR spectra of the DTC-C12, PM6:PY-C11 and PM6:PY-C11 (DTC-C12) blend films before and after thermal annealing.

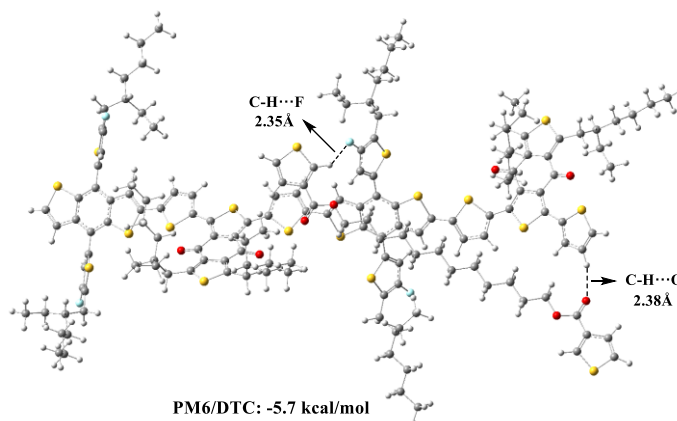


Fig. S16 The binding structures and energies of PM6/DTC-C12 (Distance in Å, energy in kcal/mol).

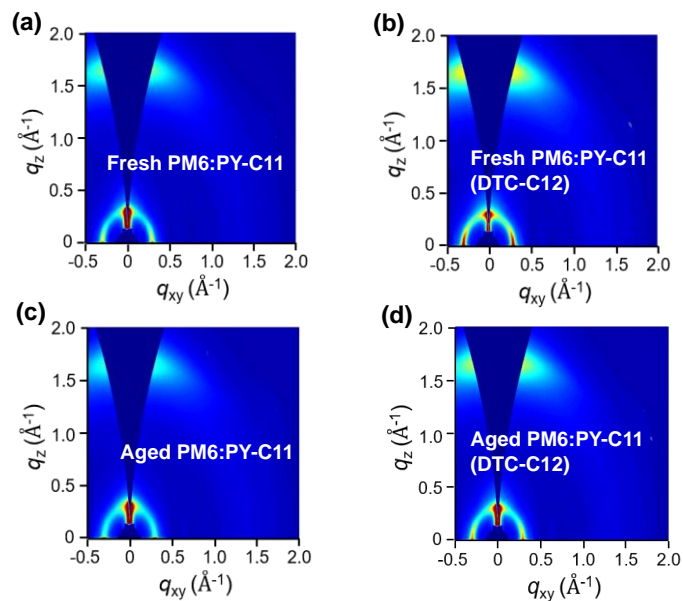


Fig. S17 2D GIWAXS diffraction patterns of the PM6:PY-C11 and PM6:PY-C11 (DTC-C12) blend films before and after LED illumination for 192 h.

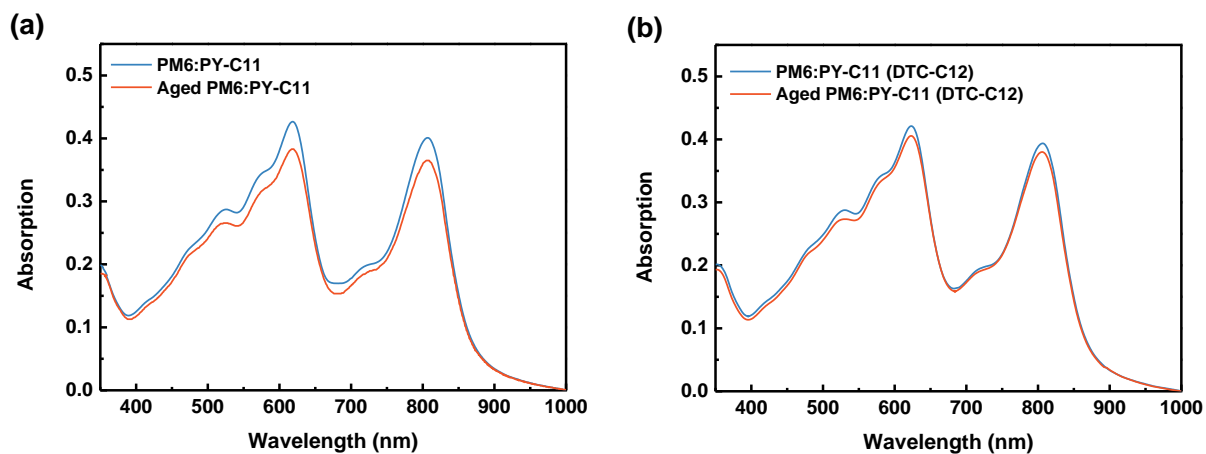


Fig. S18 UV-Vis absorption of the PM6:PY-C11 and PM6:PY-C11 (DTC-C12) blends before and after LED illumination for 192 h.

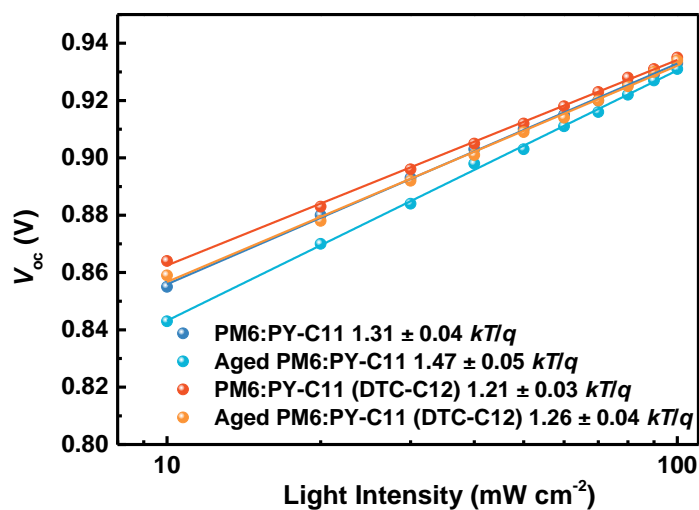


Fig. S19 The light intensity dependence V_{oc} of PM6:PY-C11 and PM6:PY-C11 (DTC-C12) devices before and after LED illumination for 192 h. The fitting slope of the curves were obtained from five independent devices.

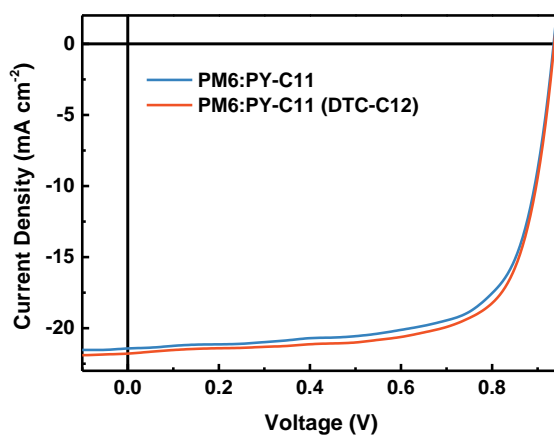


Fig. S20 The J - V characteristics of flexible PM6:PY-C11 devices processed without and with DTC-C12.

Table S1. Crystal coherence length and the d -spacing of (010) peaks in OOP direction and (100) peaks in IP direction of PM6 and PY-C11 neat films processed without DTC additives and with DTC-C8, DTC-C12 and DTC-C16.

Neat film	010 (OOP)				100 (IP)			
	q (\AA^{-1})	d -spacing (\AA^{-1})	FWHM (\AA^{-1})	CCL (\AA)	q (\AA^{-1})	d -spacing (\AA^{-1})	FWHM (\AA^{-1})	CCL (\AA)
PM6	1.66	3.78	0.256	22.07	0.286	21.96	0.062	91.13
PM6 (DTC-C8)	1.67	3.76	0.231	24.46	0.286	21.96	0.050	113.00
PM6 (DTC-C12)	1.67	3.76	0.221	25.56	0.285	22.03	0.049	115.31
PM6 (DTC-C16)	1.67	3.76	0.216	26.16	0.287	21.88	0.049	115.31
PY-C11	1.59	3.95	0.249	22.69	0.344	18.25	0.128	44.14
PY-C11 (DTC-C8)	1.58	3.97	0.247	22.87	0.342	18.36	0.131	43.12
PY-C11 (DTC-C12)	1.59	3.95	0.246	22.96	0.348	18.05	0.129	43.79
PY-C11 (DTC-C16)	1.59	3.95	0.250	22.60	0.345	18.20	0.129	43.79

Table S2. Charge mobilities of PM6:PY-C11 based blends processed without DTC additives and with DTC-C8, DTC-C12 and DTC-C16.

Blend film	μ_h^a ($10^{-4} \text{ cm}^2 \text{ V}^{-1} \text{ s}^{-1}$)	μ_e^a ($10^{-4} \text{ cm}^2 \text{ V}^{-1} \text{ s}^{-1}$)	μ_h/μ_e
PM6:PY-C11	5.56 ± 0.29	4.51 ± 0.35	1.23
PM6:PY-C11 (DTC-C8)	6.17 ± 0.23	5.52 ± 0.20	1.12
PM6:PY-C11 (DTC-C12)	6.35 ± 0.27	5.95 ± 0.19	1.07
PM6:PY-C11 (DTC-C16)	7.50 ± 0.21	5.88 ± 0.27	1.27

^a Average value from independent 10 devices.

Table S3. The surface tensions of PM6 and PY-C11 neat films processed without DTC additives and with DTC-C8, DTC-C12 and DTC-C16.

Neat film	Water (°)	Glycerol (°)	γ (mN m ⁻¹)	χ
PM6	104.68	89.99	22.9	0.30
PY-C11	99.11	81.78	28.4	
PM6 (DTC-C8)	102.05	88.78	22.6	0.42
PY-C11 (DTC-C8)	99.75	81.09	29.2	
PM6 (DTC-C12)	100.51	88.61	22.2	0.59
PY-C11 (DTC-C12)	99.87	80.58	30.0	
PM6 (DTC-C16)	99.75	88.71	21.9	0.97
PY-C11 (DTC-C16)	100.51	79.72	32.1	

Table S4. Crystal coherence length and the d -spacing of (010) peaks in OOP direction and (100) peaks in IP direction of the PM6:PY-C11 and PM6:PY-C11 (DTC-C12) blends before and after LED illumination for 192 h.

Blend film	010 (OOP)				100 (IP)			
	q (Å ⁻¹)	d -spacing (Å ⁻¹)	FWHM (Å ⁻¹)	CCL (Å)	q (Å ⁻¹)	d -spacing (Å ⁻¹)	FWHM (Å ⁻¹)	CCL (Å)
PM6:PY-C11	1.62	3.88	0.266	21.24	0.291	21.58	0.057	99.12
PM6:PY-C11 (DTC-C12)	1.63	3.85	0.249	22.69	0.289	21.73	0.051	110.78
Aged PM6:PY-C11	1.62	3.88	0.291	19.42	0.290	21.66	0.076	74.34
Aged PM6:PY-C11 (DTC-C12)	1.63	3.85	0.263	21.49	0.292	21.51	0.056	100.89

Table S5. Photovoltaic parameters of flexible PM6:PY-C11 devices processed without and with DTC-C12.

Active layer	V_{oc} (V)	J_{sc} (mA cm ⁻²)	FF (%)	PCE ^a (%)
PM6:PY-C11	0.931 (0.929 ± 0.001)	21.43 (21.15 ± 0.20)	70.3 (69.6 ± 0.7)	14.03 (13.69 ± 0.21)
PM6:PY-C11 (DTC-C12)	0.933 (0.932 ± 0.001)	21.79 (21.68 ± 0.24)	71.8 (70.8 ± 0.8)	14.60 (14.31 ± 0.20)

^aAverage value obtained from five independent devices.

References

1. J. Song, C. Li, J. Qiao, C. Liu, Y. Cai, Y. Li, J. Gao, M. H. Jee, X. Hao, H. Y. Woo, Z. Tang, H. Yan and Y. Sun, *Matter*, 2023, **6**, 1542-1554.
2. Y. Li, Q. Li, Y. Cai, H. Jin, J. Zhang, Z. Tang, C. Zhang, Z. Wei and Y. Sun, *Energy Environ. Sci.*, 2022, **15**, 3854-3861.
3. Y. Li, J. Song, Y. Dong, H. Jin, J. Xin, S. Wang, Y. Cai, L. Jiang, W. Ma, Z. Tang and Y. Sun, *Adv. Mater.*, 2022, **34**, 2110155.
4. H. Yu, M. Pan, R. Sun, I. Agunawela, J. Zhang, Y. Li, Z. Qi, H. Han, X. Zou, W. Zhou, S. Chen, J. Y. L. Lai, S. Luo, Z. Luo, D. Zhao, X. Lu, H. Ade, F. Huang, J. Min and H. Yan, *Angew. Chem. Int. Ed.*, 2021, **60**, 10137-10146.
5. L. Zhang, X. Zhu, D. Deng, Z. Wang, Z. Zhang, Y. Li, J. Zhang, K. Lv, L. Liu, X. Zhang, H. Zhou, H. Ade and Z. Wei, *Adv. Mater.*, 2022, **34**, 2106316.